REPORT DOCUMENTATION PAGE

Form Approved
OMB No. 0704-0188

1. AGENCY USE ONLY *(Leave blank)*	2. REPORT DATE	3. REPORT TYPE AND DATES COVERED
	12 July 2002	Final

4. TITLE AND SUBTITLE
Fuzzy Logic Based Image Fusion

5. FUNDING NUMBERS
PE

6. AUTHOR(S)
Thomas Meitzler, David Bednarz, Euijung Solun, Kimberly Lane, Darryl Bryk, Gulsheen Kaur, Harpreet Singh, Samuel Ebenstein, Gregory H Smith, Yelena Rodin, James S. Rankin II

7. PERFORMING ORGANIZATION NAME(S) AND ADDRESS(ES)
Survivability Technology Area
Visual Perception Laboratory
US Army TACOM

8. PERFORMING ORGANIZATION REPORT NUMBER
13818

9. SPONSORING/MONITORING AGENCY NAME(S) AND ADDRESS(ES)
NA

10. SPONSORING/MONITORING AGENCY REPORT NUMBER
NA

11. SUPPLEMENTARY NOTES
NA

12a. DISTRIBUTION AVAILABILITY STATEMENT
Unclassified/Unlimited

12b. DISTRIBUTION CODE

13. ABSTRACT *(Maximum 200 words)*

The fusion of visual and infrared sensor images of potential driving hazards in static infrared and visual scenes is computed using the Fuzzy Logic Approach (FLA). The FLA is presented as a new method for combining images from different sensors for achieving an image that displays more information than either image separately. Both Mamdani and ANFIS methods are used. The fused sensor images are compared to metrics to measure the increased perception of a driving hazard in the sensor-fused image. The metrics are correlated to experimental ranking of the image quality. The image rankings are obtained by presenting imagery in the TARDEC Visual Perception Lab (VPL) to subjects. Probability of detection of a driving hazard is computed using data obtained in observer tests.

14. SUBJECT TERMS
Fuzzy logic, Image fusion, Infrared sensors, visual sensors

15. NUMBER OF PAGES
7

16. PRICE CODE

17. SECURITY CLASSIFICATION OF REPORT	18. SECURITY CLASSIFICATION OF THIS PAGE	19. SECURITY CLASSIFICATION OF ABSTRACT	20. LIMITATION OF ABSTRACT
Unclassified		Unclassified	SAR

13818

OPSEC REVIEW CERTIFICATION

(AR 530-1, Operations Security)

I am aware that there is foreign intelligence interest in open source publications. I have sufficient technical expertise in the subject matter of this paper to make a determination that the net benefit of this public release outweighs any potential damage.

Reviewer: Steven Schehr | 15 | AD | _____
Name | Grade | Title | Uses

Steven Schehr | 4-26-02
Signature | Date

Description of Information Reviewed:

Title: Fuzzy Logic Base Image Fusion

Author/Originator(s): Mitzler et. al.

Publication/Presentation/Release Date: July 02

Purpose of Release: Technical paper

An abstract, summary, or copy of the information reviewed is available for review.

Reviewer's Determination (circle one):

(1. Unclassified Unlimited.)

2. Unclassified Limited, Dissemination Restrictions IAW_____

3. Classified. Cannot be released, and requires classification and control at the level of _____.

Security Office (AMSTA-CS-S):

(Concur)/Nonconcur _____ 29 JUL 02
Signature | Date

Public Affairs Office (AMSTA-CS-CT):

(Concur)/Nonconcur _____ 30 Jul 02
Signature | Date

Fuzzy Logic Based Image Fusion

Thomas J. Meitzler*[a], Member, IEEE, David Bednarz[a], E.J. Sohn[a], Kimberly Lane[a], Darryl Bryk
Gulsheen Kaur[b], Harpreet Singh[b],
Samuel Ebenstein[c], Gregory H. Smith[c], Yelena Rodin[c], James S. Rankin II[c]

[a]U.S. Army TACOM, AMSTA-TR-R, MS263, Warren, MI, 48397-5000
[b]Wayne State University, ECE Dept., Detroit, MI
[c]FORD Motor Company, Scientific Research Laboratory, Dearborn, MI

Abstract--**The fusion of visual and infrared sensor images of potential driving hazards in static infrared and visual scenes is computed using the Fuzzy Logic Approach (FLA). The FLA is presented as a new method for combining images from different sensors for achieving an image that displays more information than either image separately. Both Mamdani and ANIFS methods are used. The fused sensor images are compared to metrics to measure the increased perception of a driving hazard in the sensor-fused image. The metrics are correlated to experimental ranking of the image quality. The image rankings are obtained by presenting imagery in the TARDEC Visual Perception Lab (VPL) to subjects. Probability of detection of a driving hazard is computed using data obtained in observer tests.**

1. INTRODUCTION

A great deal of interest has been shown in applying the FLA during the last three decades since the initial idea by Zadeh [1,2, 3, 4, 5, 6, 7]. A strong point of the FLA is that it permits the encoding of expert knowledge directly and easily using rules with linguistic labels. A week point is that it usually takes some time to design and tune the membership functions that quantitatively define these linguistic parameters of interest. To enable a system to deal with cognitive uncertainties in a manner more like humans, researchers have incorporated the concept of fuzzy logic into many control systems. It has been found that artificial neural network learning techniques can automate this process and substantially reduce development time while improving performance. The integration of this technique with the Neuro-Fuzzy Approach is called ANFIS and an example of this processing is also shown.[1]

2. METHOD

The source imagery for fusion was obtained by capturing "stills" from AVI movies prepared for a photosimulation test that compared the observer probability of detection (Pd) of visual versus infrared imagery bands for driving hazards [9]. The images were then combined by a FLA MATLAB Fuzzy Inference System (FIS). In his book Multi-Sensor Fusion [10], Brooks points out that Fuzzy logic is a technology that shows "promise for use with sensor problems." He goes on to mention, however, that because of the numerous forms of membership functions, methods of recombination, etc., it is difficult to know exactly which implementation is best suited for use in sensor fusion technology. The authors in this paper discuss one such method. The algorithm for the method used is shown below.

An experiment was designed using two levels for scene, two levels for noise, two levels for fog, three levels for IR contrast, and three levels for sensor. Since subjects vary in their ability to perceive objects they will be treated as a blocking factor. Not all permutations of the factors are possible. Once a subject is chosen the order in which the treatment pictures are shown is randomly determined. Thus we have a 2 X 2 X 2 X 3 X 3 factorial experiment run in a randomized incomplete block.

The algorithm for pixel level image fusion using Mamdani Fuzzy Logic is:

- Read first image in variable i1 and find its size (rows: z1, columns: s1).
- Read second image in variable i2 and find its size (rows: z2, columns: s2).
- Variables i1 and i2 are images in matrix form where each pixel value is in the range from 0-255. Use Gray Colormap.
- Compare rows and columns of both input images, starting from the upper left. If the two images are not of the same size, select the portion which are of same size.
- Convert the images in column form which has C= z1*s1 entries.
- Make a FIS file which has two input images.
- Decide number and type of membership functions for both the input images by tuning the membership

[1] Further author information -
T.J.M. (correspondence): Email: meitzlet@cc.tacom.army.mil; Telephone: (810)574-5405; Fax (810)574-6145

functions. Input images in antecedent are resolved to a degree of membership between 0 to 255.

- Make rules for two input images which resolves the two antecedents to a single number from 0 to 255.
- For num=1 to C in steps of one, apply fuzzification using the rules developed above on the corresponding pixel values of the input images which gives a fuzzy set represented by a membership function and results in output image in column format.
- Convert the column form to matrix form and display the fused image.

3. DATA

In Figures 1a through 3c below are samples of the various input images used and the combined output using the FLA. Pictures of the FLA FIS are also shown below in the figures. Fig.'s 1a, 1b and 1c are the white-hot IR, visible, and fused images in clear condition respectively of a crossing scene. Fig.'s 2a, 2b, and 2c are of the same images but this time with gaussian noise added. Fig.'s 3a, 3b, and 3c are the same scene but using a black hot contrast setting on the infrared camera. The images show a pedestrian at a crossing at night. In Fig.'s 1b ,2b, and 3b, the stop sign, road edges and shoes can be seen, but, the pedestrian is barely visible. In Fig.'s 1a, 2a, and 3a, the infrared image of the same scene, the whole figure of the pedestrian can be seen however the Stop sign cannot be seen. Fig.'s 1c, 2c, and 3c show the fused images in which all features are visible.

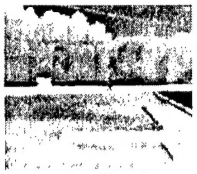
Fig. 1a

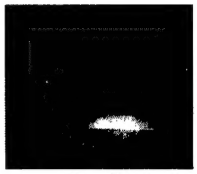
Fig. 1b

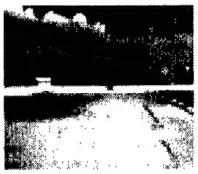
Fig. 1c


Fig. 2a

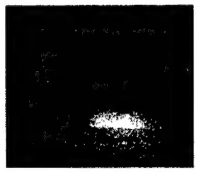
Fig. 2b


Fig. 2c


Fig. 3a


Fig. 3b

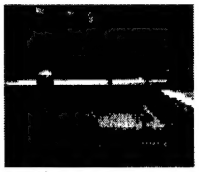
Fig. 3c

Fig.'s 4a through 6c below are in same order as above in terms of effects added but are of a different scene.

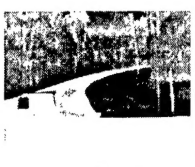
Fig.4a


Fig. 4b

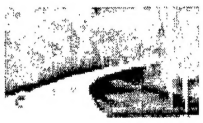
Fig 4c


Fig. 5a

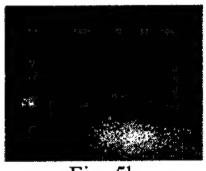
Fig. 5b


Fig. 5c


Fig. 6a


Fig.6b


Fig. 6c

Diagrams of the Mandami FIS used by the authors to fuse the images in the paper are shown below in Fig. 7, 8, and 9.

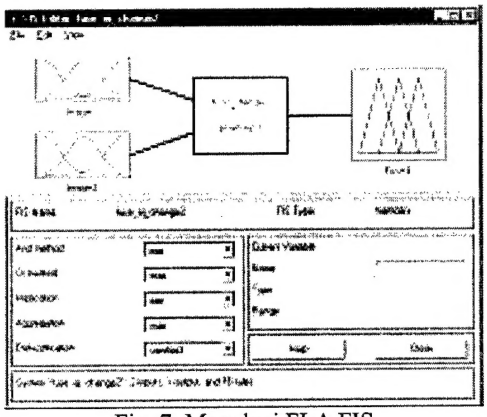
Fig. 7: Mamdani FLA FIS

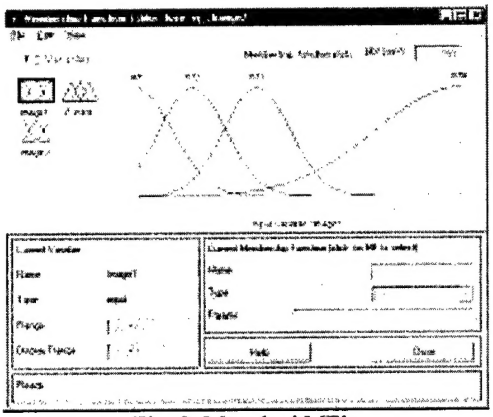
Fig. 8: Mamdani MF's

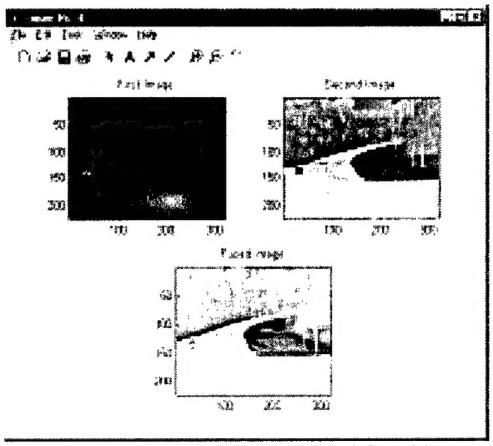

Fig. 9: Closed road visible, IR, and fused image

The ANFIS technique was also used. Below is the algorithm for sensor fusion using ANFIS. Figures 10 and 11, are the ANFIS control GUI's and Fig.'s 12a through 13c are from the ANFIS fusion of the images.

Algorithm for pixel level image fusion using ANFIS:

- Read first image in variable i1 and find its size (rows: z1, columns: s1).
- Read second image in variable i2 and find its size (rows: z2, columns: s2).
- Variables i1 and i2 are images in matrix form where each pixel value is in the range from 0-255. Use Gray Colormap.
- Compare rows and columns of both input images. If the two images are not of the same size, select the portion which are of same size.
- Convert the images to column form which has C= z1*s1 entries.
- Form a training data which is a matrix with three columns and entries in each column are from 0 to 255 in steps of 1.
- Form a check data which is a matrix of pixels of two input images in column format.
- Decide number and type of membership functions for both the input images.
- For training we need FIS structure which is generated by genfis1 command with training data, number of membership functions and type of membership functions as input.
- To start training, anfis command is used which takes generated FIS structure and training data as input and returns trained data.
- For num=1 to C in steps of one, apply fuzzification using the generated FIS structure with Check data and trained data as inputs which returns output image in column format.
- Convert the column form to matrix form and display the fused image.

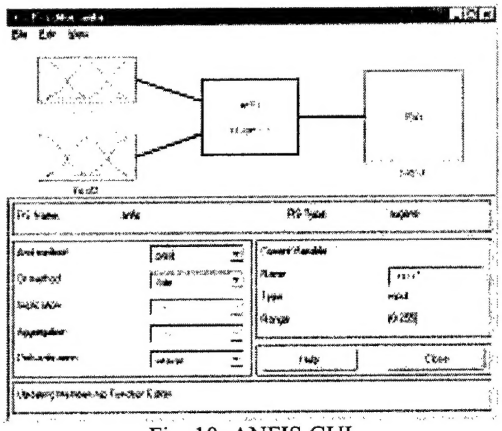

Fig. 10: ANFIS GUI

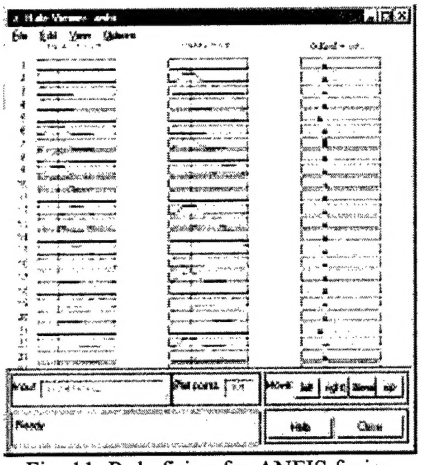

Fig. 11: Rule firing for ANFIS fusion

Fig. 12a

Fig. 12b

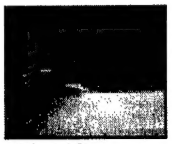

Fig. 12c

Fig. 13a

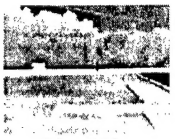

Fig. 13b

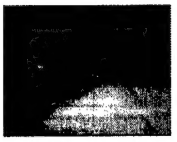

Fig. 13c

4. ANALYSIS

A texture based clutter metric was run over the images to see if there was a correlation of the experimental ranking of the quality of the imagery with a texture based clutter metric. Specifically, a normalized textured clutter metric [12] was computed for each image using a cell size that is

representative of a pedestrian and compared to the experimental detection values. An ANOVA was performed on various image set factors and experimental image ratings to determine the relationship that exists between the factors in the perception experiment. Since the original dependent variable was measured on an ordinal scale a rank transformation was applied to it. The procedure replaces the observations by their ranks. The complete analysis of variance for this experiment is summarized in Table IV. The table indicates the main effect sensor and the scene * sensor interaction are significant. Table V contains the estimated means and confidence intervals for the rank of test ratings for each sensor by scene. Table VI shows the pairwise comparisons of the main effect sensor within each scene. The mean difference is significant at the Table V contains the estimated means and confidence intervals for the rank of test ratings for each sensor by scene. Table VI shows the pairwise comparisons of the main effect sensor within each scene. The mean difference is significant at the .05 level for all the comparisons. Thus, we conclude that the performance of the three sensors is different for each scene. Table VII summarizes the univariate tests of the main effect sensor within each scene. The F test indicates that the main effect sensor is significant for each scene. The normal probability and diagnostic plots revealed no serious model violations.
Table V contains the estimated means and confidence intervals for the rank of test ratings for each sensor by scene. Table VI shows the pairwise comparisons of the main effect sensor within each scene. The mean difference is significant at the .05 level for all the comparisons. Thus, we conclude that the performance of the three sensors is different for each scene. Table VII summarizes the univariate tests of the main effect sensor within each scene. The F test indicates that the main effect sensor is significant for each scene. The normal probability and diagnostic plots revealed no serious model violations.

A Schmeider-Weathersby clutter metric and texture clutter metric [12] were applied to the fused images. The imagery in the data set was also ranked by a photosimulation experiment in the TARDEC visual perception lab. The tables below show the metrics of each image and the qualitative relative ranking of the image quality by observers. Scene one refers to the scene of the closed road and scene two is the pedestrian crossing the road. Fig.'s 13 and 14 show the linear correlation between the texture metrics and experimental scene ranking.

Table I: Visible images and clutter metrics

Scene	name	Rating	Text Clutter	Clutter
1	clear	3.17	47.33	33.45
	fog	2.92	14.33	10.18
	clear	3.17	47.33	33.45
	fog	2.92	14.33	10.18
	clear-noise	2.67	59.41	35.40
	clear-noise	2.67	59.41	35.40
	fog-noise	0.67	48.07	23.97
	fog-noise	0.67	48.07	23.97
2	clear	2.17	27.70	20.90
	fog	1.5	9.614	8.227
	clear	2.17	27.70	20.90
	fog	1.5	9.614	8.227
	clear-noise	1.5	42.13	24.35
	clear-noise	1.5	42.13	24.35
	fog-noise	0.08	39.89	19.51
	fog-noise	0.08	39.89	19.51

Table II: IR images and clutter metrics

Scene	name	Rating	Text Clutter	Clutter
1	bhot	3.58	105.4	61.36
	bhot-fog	3.42	36.44	22.10
	whot	3.5	100.9	61.07
	whot-fog	3.25	36.76	22.38
	bhot-noise	3.42	103.3	60.04
	whot-noise	3.25	103.5	60.46
	whot+fog+noise	2.42	60.15	31.51
	bhot+fog+noise	2.58	59.85	31.22
2	bhot	2.92	56.25	31.51
	bhot-fog	2.67	20.04	11.80
	whot	3	57.35	31.98
	whot-fog	2.42	20.46	12.23
	bhot-noise	2.58	60.53	32.28
	whot-noise	2.58	62.12	32.77
	whot+fog+noise	1.58	40.14	19.78
	bhot+fog+noise	1.33	38.71	19.19

Table III: Fused images and clutter metrics

Scene	Fused Rating	Fused Text Clutter	Fused Clutter
1	3.5	86.42	46.17
	3.08	32.95	17.58
	3.33	92.22	52.77
	3.08	41.57	24.44
	3	91.42	48.49
	2.92	92.15	51.36
	2.33	58.38	30.38
	2.25	51.87	25.72
2	3.33	50.46	30.49
	2.5	21.62	12.69
	3.08	52.41	29.16
	2.08	17.61	11.52
	2.67	56.84	31.10
	2.67	55.79	29.22
	1	37.52	18.88
	1.25	38.71	20.29

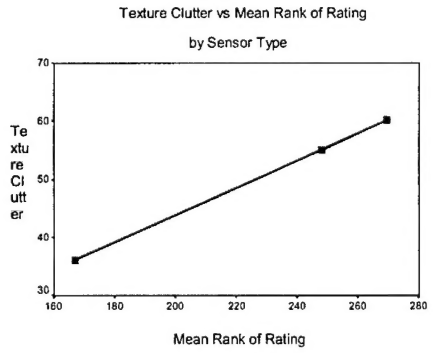

Fig. 14: Textured clutter metric vs. Pd of all sensors and subjects

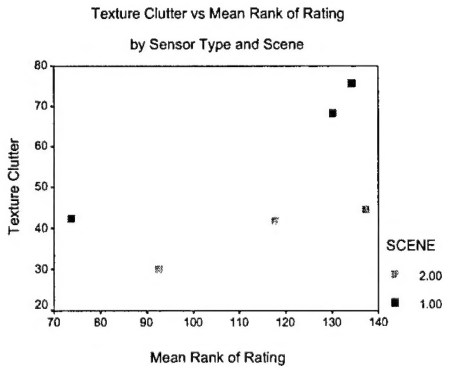

Fig. 15: Textured clutter vs mean rank by scene

Table IV: ANOVA of ranking test

Tests of Between-Subjects Effects

Dependent Variable: RANK of TEST_RAT

Source	Type IV Sum of Squares	df	Mean Square	F	Sig.
Corrected Model	6597770.924[a]	96	68726.780	15.226	.000
Intercept	21997980.5	1	21997980.47	4873.654	.000
SUBJECT	980115.137	11	89101.376	19.740	.000
SCENE	690900.033	1	690900.033	153.069	.000
NOISE	1023022.005	1	1023022.005	226.651	.000
FOG	1032900.033	1	1032900.033	228.839	.000
IR_CONTR	25187.760	1	25187.760	5.580	.019
SENSOR	43562.760	1	43562.760	9.651	.002
SUBJECT * SCENE	949697.917	11	86336.174	19.128	.000
SUBJECT * NOISE	241706.198	11	21973.291	4.868	.000
SUBJECT * FOG	102767.448	11	9342.495	2.070	.022
SUBJECT * IR_CONTR	38904.036	11	3536.731	.784	.657
SUBJECT * SENSOR	82910.286	11	7537.299	1.670	.078
SCENE * NOISE	6056.302	1	6056.302	1.342	.247
SCENE * FOG	31931.719	1	31931.719	7.074	.008
SCENE * IR_CONTR	575.260	1	575.260	.127	.721
SCENE * SENSOR	19266.667	1	19266.667	4.269	.039
NOISE * FOG	126425.208	1	126425.208	28.010	.000
NOISE * IR_CONTR	6378.190	1	6378.190	1.413	.235
NOISE * SENSOR	891.211	1	891.211	.197	.657
FOG * IR_CONTR	504.167	1	504.167	.112	.738
FOG * SENSOR	8251.042	1	8251.042	1.828	.177
IR_CONTR * SENSOR	2375.065	1	2375.065	.526	.469
Error	1728729.076	383	4513.653		
Total	36089820.0	480			
Corrected Total	8326500.000	479			

a. R Squared = .792 (Adjusted R Squared = .740)

Table V: Ranking of imagery by sensor

Estimates

Dependent Variable: RANK of TEST_RAT

SCENE	SENSOR	Mean	Std. Error	95% Confidence Interval	
				Lower Bound	Upper Bound
1	1	113.937[a]	9.697	94.871	133.004
	2	228.964[a]	6.857	215.482	242.445
	3	221.828[a]	6.857	208.346	235.310
2	1	219.875[a]	9.697	200.809	238.941
	2	310.135[a]	6.857	296.654	323.617
	3	274.667[a]	6.857	261.185	288.149

a. Based on modified population marginal mean.

Table VI: Comparison of sensors

Pairwise Comparisons

Dependent Variable: RANK of TEST_RAT

SCENE	(I) SENSOR	(J) SENSOR	Mean Difference (I-J)	Std. Error	Sig.[a]	95% Confidence Interval for Difference[a]	
						Lower Bound	Upper Bound
1	1	2	-115.026*[b]	11.877	.000	-138.377	-91.675
		3	-107.891*[b]	11.877	.000	-131.242	-84.539
	2	1	115.026*[b]	11.877	.000	91.675	138.377
		3	7.135[b]	9.697	.462	-11.931	26.202
	3	1	107.891*[b]	11.877	.000	84.539	131.242
		2	-7.135[b]	9.697	.462	-26.202	11.931
2	1	2	-90.260*[b]	11.877	.000	-113.612	-66.909
		3	-54.792*[b]	11.877	.000	-78.143	-31.440
	2	1	90.260*[b]	11.877	.000	66.909	113.612
		3	35.469*[b]	9.697	.000	16.402	54.535
	3	1	54.792*[b]	11.877	.000	31.440	78.143
		2	-35.469*[b]	9.697	.000	-54.535	-16.402

Based on estimated marginal means

*. The mean difference is significant at the .05 level.

a. Adjustment for multiple comparisons: Least Significant Difference (equivalent to no adjustments).

b. An estimate of the modified population marginal mean (I).

c. An estimate of the modified population marginal mean (J).

Table VII: Univariate Table

Univariate Tests

Dependent Variable: RANK of TEST_RAT

SCENE		Sum of Squares	df	Mean Square	F	Sig.
1	Contrast	479485.5	2	239742.773	53.115	.000
	Error	1728729	383	4513.653		
2	Contrast	262370.6	2	131185.286	29.064	.000
	Error	1728729	383	4513.653		

Each F tests the simple effects of SENSOR within each level combination of the other effects shown. These tests are based on the linearly independent pairwise comparisons among the estimated marginal means.

In addition to the clutter metrics, an Entropy the pictures were evaluated using an Entropy metric [12]. The entropy of an image is a measure of the information content, in terms of gray scale levels and is also related to the texture of the image. The maximum value the entropy metric can take on is eight and the minimum is zero. The equation used for the calculation of the entropy is shown below,

$$H = -\sum_{g=0}^{L-1} p(g)\log_2 p(g)$$

where p(g) is he probability of gray value g, and the range of g is [0,...,L-1].

Table VIII. Significance of Entropy to other variables

Tests of Between-Subjects Effects

Dependent Variable: ENTROPY

Source	Type IV Sum of Squares	df	Mean Square	F	Sig.
Corrected Model	31.928[a]	6	5.321	15.886	.000
Intercept	1461.996	1	1461.996	4364.644	.000
SCENE	.659	1	.659	1.967	.170
NOISE	8.598	1	8.598	25.668	.000
FOG	13.513	1	13.513	40.343	.000
IR_CONTR	1.970E-02	1	1.970E-02	.059	.810
SENSOR	.411	1	.411	1.227	.276
Error	11.054	33	.335		
Total	1747.769	40			
Corrected Total	42.982	39			

a. R Squared = .743 (Adjusted R Squared = .696)

Table VIII above shows that the scene, noise and fog variables are significant to the entropy value. The type of sensor used was not significant to entropy, this was surprising. Fig. 16 below shows graphically how the sensors ranked by entropy.

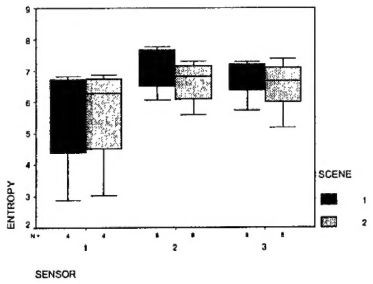

Fig. 16: Mean Ranking of Sensor by Entropy

Table VIII above shows that the scene, noise and fog variables are significant to the entropy value. The type of sensor used was not significant to entropy, this was surprising. The figure below shows how the texture clutter correlated to the entropy values. Fig. 17 shows that the entropy metric is linearly correlated to texture, but not as sensitive.

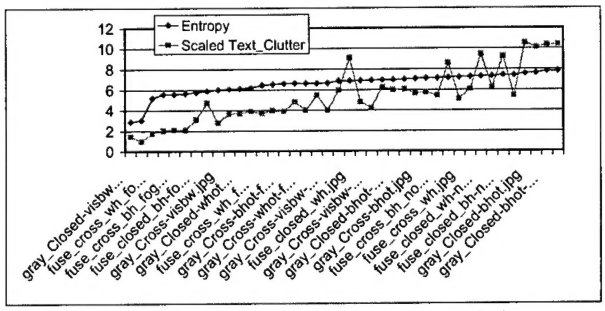

Fig. 17: Correlation of Entropy to textured clutter

5. CONCLUSIONS

The authors have introduced procedures for using Mamdani and neural network based Fuzzy Logic algorithms to execute sensor fusion of images in the visual and infrared part of the spectrum. The analysis of the experimental data and interactions between subjects shows, as expected that the initial scenes are very important to the quality of the fused image. For night driving, since the visual scene will always be low contrast, the fused image cannot be much better in terms of computer based image metrics that measure image quality, than the IR image. The fused imagery, however, may contain features that are recognizable to a person and not the

metric, such as the presence of the stop sign in the one set of the data. More work will be done to increase the robustness of the FIS used to perform the sensor fusion. A combination of enhancing spatial filters and or processing used in combination with the sensor fusion would improve the quality of the visible image and therefore the fused image. A matched filter algorithm was used on some of the images to estimate the practicality of using the matched-filter approach to target recognition problems. The benefit of using the Fuzzy Logic Approach in image sensor fusion is that simple rules can be exploited to achieve the fusion of several bands.

There are military applications of sensor fusion. Below is a figure of an IR, Fig. 18a, and visible image, Fig. 18b, of a tank against a smoke-covered terrain. The image in Fig. 18c is fused using the FIS and contains image features common to both of the original pictures.

Fig: 18a IR

Fig. 18b:visible

Fig. 18c: fused

REFERENCES

[1]. L. Zadeh, "Fuzzy Sets", Information and Control", 8, pp. 338-353, 1965.

[2]. E. Mamdani and S. Assilian, "Applications of fuzzy algorithms for control of simple dynamic plant", Proc. Inst. Elec. Eng., Vol. 121, pp. 1585-1588, 1974.

[3]. T. Munakata, and Y. Jani, "Fuzzy Systems: An Overview", Commun., ACM, Vol. 37, No. 3, pp. 69-76, Mar. 1994.

[4]. R. Mizoguchi, and H. Motoda (eds.), "AI in Japan: Expert Systems Research in Japan", IEEE Expert, pp. 14-23, Aug. 1995.

[5]. E. Cox, ***The Fuzzy Systems Handbook: A Practitioner's Guide to Building, Using, and Maintaining Fuzzy Systems***, AP Professional, 1994.

[6]. D. G. Schwartz, G. J. Klir, H. W. Lewis, and Y. Ezawa, "Applications of Fuzzy Sets and Approximate Reasoning", IEEE Proc., Vol. 82, No. 4, pp. 482-498, Apr. 1994.

[7]. T. Terano, K. Asai, and M. Sugeno, *Fuzzy Systems and its Applications*, AP Professional, 1992.

[8]. J-S. R. Jang, "ANFIS: Adaptive-Network-Based Fuzzy Inference System", IEEE Trans. Sys., Man, and Cyber., Vol. 23, No. 3, pp. 665-684, May/Jun. 1993.

[9]. Meitzler, T., Bednarz, D., Lane, K., Bryk, D., Sohn, E.J., Jusela, D., Ebenstein, S., Smith, G., and Rodin, Y., "Noise and Contrast Comparison of Visual and Infrared Images of Hazards as Seen Inside an Automobile", Proceedings of SPIE's 14th Annual International Symposium on Aerospace Defense Sensing, Enhanced and Synthetic Vision 2000, SPIE Vol. 4023, April 2000.

[10.]. R.R. Brooks, S.S. Iyengar, ***Multi-Sensor Fusion: Fundamentals and Applications with Software***, Prentice Hall PTR, Upper Saddle River, N. J., p. 167, 1997

[11]. Meitzler, T., Jackson, W., Bednarz, D., Sohn, E., "Calculation of background clutter in infrared imagery: a semi-empirical study," Proceedings of the Targets and Background Characterization, SPIE Symposium, April, 1993.

[12]. Wang,Y., Lohmann, B., "Multisensor Image Fusion: Concept, Method and Applications.